Identification of Separate Structural Features That Affect Rate and Cation Concentration Dependence of Self-Cleavage by the *Neurospora* VS Ribozyme†

Alan H. L. Poon, Joan E. Olive, Meredith McLaren, and Richard A. Collins*

Department of Molecular and Medical Genetics, University of Toronto, 1 Kings College Circle, Toronto, Ontario M5S 1A8, Canada

Received April 20, 2006; Revised Manuscript Received August 22, 2006

ABSTRACT: The cleavage site of the *Neurospora* VS ribozyme is located in an internal loop in a hairpin called stem-loop I. Stem-loop I undergoes a cation-dependent structural change to adopt a conformation, termed shifted, that is required for activity. Using site-directed mutagenesis and kinetic analyses, we show here that the insertion of a single-stranded linker between stem-loop I and the rest of the ribozyme increases the observed self-cleavage rate constant by 2 orders of magnitude without affecting the Mg^{2+} requirement of the reaction. A distinct set of mutations that favors the formation of the shifted conformation of stem-loop I decreases the Mg^{2+} requirement by an order of magnitude with little or no effect on the observed cleavage rate under standard reaction conditions. Similar trends were seen in reactions that contained Li^{+} instead of Mg^{2+}. Mutants with lower ionic requirements also exhibited increased thermostability, providing evidence that the shifted conformation of stem-loop I favors the formation of the active conformation of the RNA. In natural, multimeric VS RNA, where a given ribozyme core is flanked by one copy of stem-loop I immediately upstream and another copy 0.7 kb downstream, cleavage at the downstream site is strongly preferred, providing evidence that separation of stem-loop I from the ribozyme core reflects the naturally evolved organization of the RNA.

The naturally occurring small ribozymes, including the hammerhead, hairpin, hepatitis delta virus, and *Neurospora* VS[1], have been used extensively as model systems to study RNA catalysis (*1*). Despite their simplicity, it has proven challenging to determine which step in the folding and catalysis process is actually being measured in the observed rate of a reaction. Moreover, the observed rate and extent of cleavage and ligation can differ substantially in different versions of a given ribozyme and in different reaction conditions. For example, minimal versions of the hammerhead and hairpin ribozyme require much higher concentrations of cations to achieve maximal cleavage rate than do those that include natural peripheral sequences (*2*−*5*).

Previous experiments with the *Neurospora* VS ribozyme have implicated helix Ia as an inhibitory structural element that limits the observed rate of the cis-cleavage reaction in the well-characterized G11 version of the ribozyme (Figure 1). For example, modification−interference experiments and site-directed mutagenesis showed that disruption of base pairing in helix Ia increased the rate of self-cleavage (*6*, *7*). A consequence of disrupting helix Ia is that the nucleotides that formerly comprised the 3′ side of the helix (nts 640−643; highlighted in bold in Figure 1a) effectively become a flexible single-stranded linker that tethers the remaining part of stem-loop I, including the site of self-cleavage, to the rest of the ribozyme (see mutant H3 in Figure 1a). We have recently found that some other versions of the VS ribozyme, especially a circular permutation that uses a long linker to tether helix I to the 3′ end of the ribozyme, have a very fast rate of self-cleavage (*8*). trans-cleaving versions of VS RNA, where stem-loop I is not covalently attached to the rest of the ribozyme, also cleave about 10-fold faster than the cis-cleaving G11 RNA from which they were derived (*9*, *10*). These observations suggest that the cleavage rate of the G11 version of VS RNA is limited by the short distance between helix Ia and the rest of the ribozyme.

In the current work, we have systematically investigated the effects on the cleavage rate of disrupting helix Ia and/or lengthening the linker between helices I and II. Our results provide evidence that the cleavage rate is increased substantially by relieving the constraint that results from the close covalent attachment of helices I and II. Also, disrupting helix Ia or making other changes that facilitate the formation of the conformation of stem-loop I that is required for activity increases the stability of the active form of the ribozyme.

EXPERIMENTAL PROCEDURES

Clones. ANX28 contains a 28 nt linker sequence inserted via oligonucleotide-directed mutagenesis between stems I and II of the G11 version of VS RNA ((*11*); Figure 1). The linker sequence was designed to minimize stable secondary structure potential and to contain unique recognition sites for restrictions enzymes AvrII, NheI, and XbaI, each of which leaves the same 4 bp overhang. This design allowed the easy construction of a series of shorter linkers of differing length

† Supported by grant MT-12837 from the Canadian Institutes of Health Research.

* To whom correspondence should be addressed. Tel: (416) 978-3541. Fax: (416) 978-6885. E-mail: rick.collins@utoronto.ca.

[1] Abbreviations: VS, Varkud satellite; nt, nucleotide.

10.1021/bi060769+ CCC: $33.50
Published on Web 10/13/2006

and sequence by digestion with pairs of enzymes followed by re-ligation. Additional sequence changes were introduced by oligonucleotide-directed mutagenesis and confirmed by DNA sequencing. Clone GAv3′Ia (Figure 7 and Supporting Information), was used to synthesize an RNA called PMD, which contains a full-length VS RNA monomer (M) flanked upstream by a T7-promoter-proximal self-cleavage fragment, designated P, containing 9 nt of vector sequence and 4 nt (617 to 620) of VS RNA, and a downstream cleavage product, designated D, containing VS nt 621−643 followed by 149 nt of pTZ19R vector sequence, when transcribed from a template linearized at the Bgl*I* site in the vector.

RNA Synthesis and Cleavage Reactions. Precursor RNAs were synthesized from linearized plasmid DNAs by *in vitro* transcription using T7 RNA polymerase and purified from denaturing polyacrylamide gels as described (*12*, *13*). RNAs were dissolved in water, and cleavage reactions were initiated by the addition of one-fifth volume of reaction solution to obtain final concentrations of 40 mM Tris-HCl at pH 8.0, 50 mM KCl, and $MgCl_2$ or monovalent salts at the concentrations indicated in the Figures. Experiments were conducted at 37 °C unless otherwise indicated. For experiments at higher temperatures, care was taken to ensure that all reagents, tubes and pipet tips remained at the specified temperature. Aliquots were removed at appropriate times and quenched with two volumes of loading dye (80% formamide, 45 mM Tris base, 45 mM boric acid, 50 mM EDTA, and 0.05% each bromophenol blue and xylene cyanol), separated by denaturing polyacrylamide gel electrophoresis, and exposed to a PhosphorImager screen and quantified using ImageQuant software (Molecular Dynamics, Sunnyvale, CA).

Data Analysis. The fraction of precursor cleaved versus time was fit to a single exponential analysis using SigmaPlot or custom Microsoft Excel macros to estimate the apparent cleavage rate constant, k (min^{-1}) and the final extent of cleavage, f_{max}, which was typically 80−90%. For each RNA, two to four replicates of each self-cleavage time course were performed at each of five to seven concentrations of $MgCl_2$. Plots of rate constant versus Mg^{2+} concentration were fit using SigmaPlot to the three-parameter Hill equation to obtain estimates of the cleavage rate constant at saturating concentrations of Mg^{2+} (k_{max}), the concentration of Mg^{2+} required to obtain half-maximal cleavage rate ($[Mg^{2+}]_{1/2}$), and the Hill coefficient (n).

RESULTS AND DISCUSSION

Stem-loop I of the self-cleaving G11 version of the VS ribozyme consists of base-paired helices Ia and Ib, separated by an internal loop that contains the site of cleavage (Figure 1a and b). Mutant H3 differs from G11 in that the 13 nucleotides upstream of the cleavage site have been replaced with three guanosines, which disrupts helix Ia and converts the nucleotides that comprise the 3′ side helix Ia in G11 into a single-stranded linker in H3 (nucleotides 640−643, highlighted in bold in Figure 1a). Cleavage of H3 was detectable at a much lower concentration of Mg^{2+} than required for G11 (1 mM Mg^{2+} vs 5 mM for G11; Figure 1c and data not shown) and reached maximal rate (k_{max}) at a lower concentration of Mg^{2+} (≈17 mM vs >100 mM for G11). At saturating Mg^{2+} concentration, H3 cleaved approximately 5-fold faster than G11 (Figure 1c). To compare the magnesium dependence of the cleavage rate among different RNAs (see also Figures 2−4), the concentration of Mg^{2+} required to reach half-maximal cleavage rate ($[Mg^{2+}]_{1/2}$) was used; by this criterion, H3 had a 5-fold lower Mg^{2+} requirement than G11; $[Mg^{2+}]_{1/2}$ values of 4.4 and 21.9 mM, respectively (Figure 1c). Also, the Hill coefficient of H3 was higher than that of G11 (3.1 ± 0.4 vs 1.7 ± 0.2, respectively), indicating a higher degree of cooperativity in binding Mg^{2+}. These trends are similar to results obtained previously with H3 in different reaction conditions (*7*) and show that disrupting

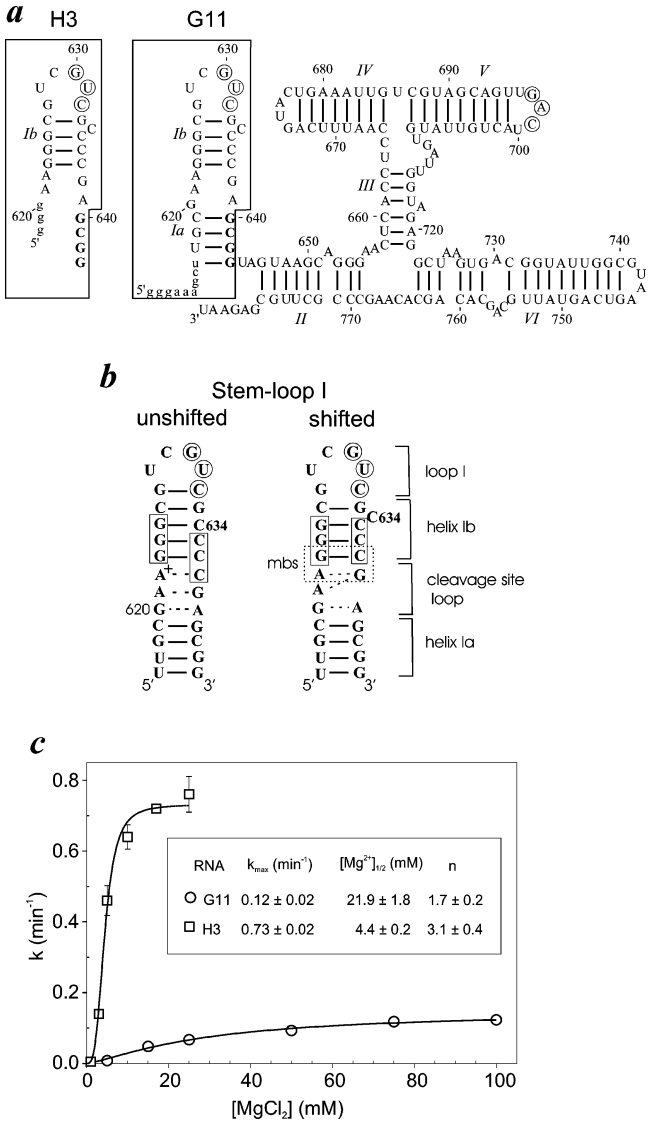

FIGURE 1: Secondary structure of the G11 and H3 versions of the VS ribozyme. (a) Helices and stem-loops are indicated by Roman numerals. Stem-loop I is enclosed in a box; the secondary structure of stem-loop I of mutant H3 is indicated to the left. The circled nucleotides form a kissing interaction between loops I and V. The site of cleavage is indicated by an arrowhead. Nucleotides 640−643 that comprise the 3′ side of helix Ia are highlighted in bold (see text). (b) Diagram of the structure of the unshifted, inactive, and shifted active conformations of helix I ((*26*−*28*); see text). A metal ion binding site (mbs; (*14*)) in the shifted conformation is boxed; (c) Effect of Mg^{2+} concentration on the cleavage rate of G11 and H3. Self-cleavage reactions were performed over a range of concentrations of Mg^{2+} and analyzed as described in Experimental Procedures. Apparent first-order rate constants, k, are plotted vs $[Mg^{2+}]$. The estimated cleavage rate constant at saturating $[Mg^{2+}]$, (k_{max}), the $[Mg^{2+}]$ required to obtain half-maximal cleavage rate, $[Mg^{2+}]_{1/2}$, and the Hill coefficient, n, are indicated.

a

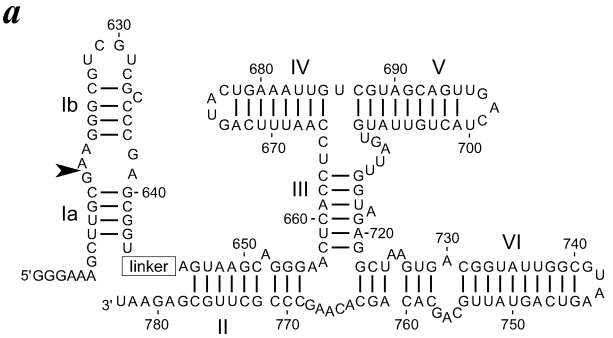

RNA	Linker Length	Linker Sequence (5' to 3')
G11-3	3	CAC
AX7	7	CACCUAG
AX11	11	CACCUAGCUAG
AN16	16	CACCUAGCAACUCUAG
ANX28	28	CACCUAGGAACAACGCUAGCAACUCUAG

b

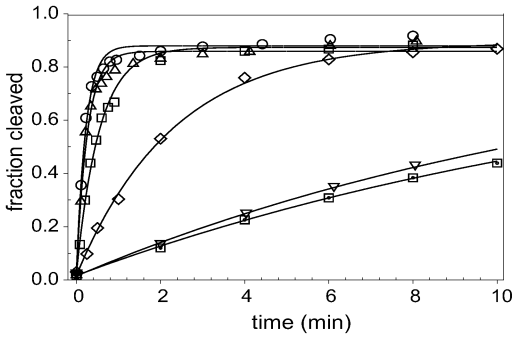

c

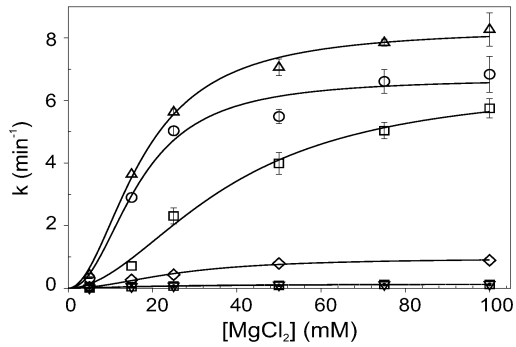

d

RNA	linker (nt)	k_{max} (min^{-1})	$[Mg^{2+}]_{1/2}$ mM	n
G11	0	0.12 ± 0.01	21.9 ± 1.8	1.7 ± 0.2
G11-3	3	0.13 ± 0.02	21.3 ± 1.7	1.7 ± 0.2
AX7	7	0.96 ± 0.07	25.8 ± 3.0	2.0 ± 0.4
AX11	11	6.5 ± 0.7	38.0 ± 6.3	1.9 ± 0.3
AN16	16	6.8 ± 0.5	16.9 ± 2.2	2.1 ± 0.6
ANX28	28	8.3 ± 0.3	17.5 ± 1.2	2.0 ± 0.3

FIGURE 2: Insertion of a linker sequence between helices I and II increases the cleavage rate. (a) A series of mutant RNAs was constructed, each containing a linker sequence of 3−28 nts inserted at the position indicated by the rectangle labeled linker (Experimental Procedures); (b) Time courses of self-cleavage of G11 and linker-containing RNAs were performed in 40 mM Tris-HCl at pH 8.0, 50 mM KCl, and 25 mM Mg^{2+} at 37 °C. Symbols are defined in d . (c) Effect of $[Mg^{2+}]$ on the cleavage rate constant of linker-containing RNAs. (d) The data in c were fit to the three-parameter Hill equation to obtain estimates of the cleavage rate constant at saturating concentrations of Mg^{2+} (k_{max}), the concentration of Mg^{2+} required to obtain half-maximal cleavage rate ($[Mg^{2+}]_{1/2}$), and the Hill coefficient (n).

helix Ia and/or introducing a flexible linker between helix I and the rest of the ribozyme affects the rate and divalent ion requirement of the self-cleavage reaction.

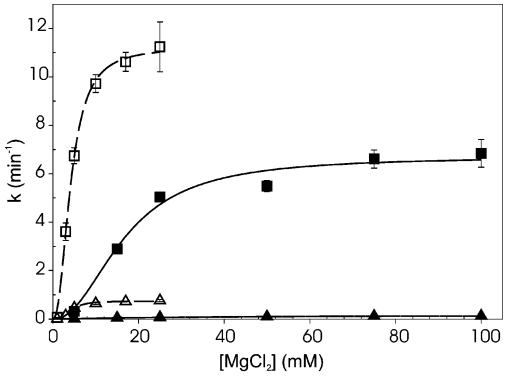

RNA	Ia	L	k_{max} (min^{-1})	$[Mg^{2+}]_{1/2}$ mM	n
▲ G11	+	-	0.12 ± 0.01	21.9 ± 1.8	1.7 ± 0.2
■ AN16	+	+	6.8 ± 0.3	16.8 ± 1.6	2.0 ± 0.4
△ H3	-	-	0.73 ± 0.2	4.4 ± 0.2	3.1 ± 0.4
□ AN16-H3	-	+	11.3 ± 0.3	4.2 ± 0.2	2.3 ± 0.3

FIGURE 3: Disrupting helix Ia lowers the Mg^{2+} requirement of the cleavage reaction. Cleavage rate constants were measured over a range of Mg^{2+} concentrations for RNAs containing (+) or lacking (−) helix Ia and/or a 16 nt linker (L) between helices Ia and II. See Figures 1 and 2 for RNA sequences; AN16-H3 is the same as H3 (Figure 1a) except that it contains the AN16 linker (Figure 2a). Data were analyzed as in Figure 2.

Insertion of a Linker between Helices Ia and II Increases the Cleavage Rate. To test the hypothesis that the differences in properties of the cleavage reaction between H3 and G11 were due to the nucleotides that comprise the 3′ side of helix Ia in G11 acting as a single-stranded linker in H3, a series of RNAs was constructed in which helix Ia was retained, and linkers of different length were inserted between helices Ia and II of G11 (Figure 2 a and b). Time courses of cleavage in the presence of 25 mM Mg^{2+} showed that the insertion of a three-nucleotide linker did not increase the cleavage rate; however, RNAs with linkers of 7, 11, or 16 nts cleaved substantially more rapidly, and an even longer linker, 28 nt, showed only a slight further increase in rate compared to that of the 16 nt linker (Figure 2c). Cleavage rates were unaffected by changes in the concentration of RNA (between 5 and 500 nM; data not shown), indicating that the reactions were indeed intramolecular cis-cleavage. Cleavage rates of each linker insertion mutant were measured over a range of Mg^{2+} concentrations. Figure 2 shows that the RNA with the 3nt linker cleaved indistinguishably from G11 under all conditions, but for the RNAs containing longer linkers, the maximal cleavage rate (k_{max}) increased substantially with increasing linker length and $[Mg^{2+}]$, reaching a maximum of approximately 7−8 min^{-1}, almost 2 orders of magnitude faster than G11. The $[Mg^{2+}]_{1/2}$ values for most of the linker insertion mutants were similar to each other (ranging from 16.8 to 25.8 mM) and not substantially different from G11 (21.9 mM); the AX11 RNA had a slightly higher $[Mg^{2+}]_{1/2}$ of 38.0 mM. Hill coefficients for all RNAs were also similar at $n \approx 2.0$. Thus, the linker insertion mutants, like the G11 RNA, had $[Mg^{2+}]_{1/2}$ values much higher than that of H3 (4.4 mM; cf. Figure 1c). We conclude that insertion of a linker into G11 increases the cleavage rate but is not sufficient to lower the Mg^{2+} requirement.

Disruption of Helix Ia Lowers the Mg^{2+} Requirement. Because H3 has a lower $[Mg^{2+}]_{1/2}$ than any of the linker insertion mutants (all of which still contain helix Ia), we hypothesized that helix Ia was the structural feature respon-

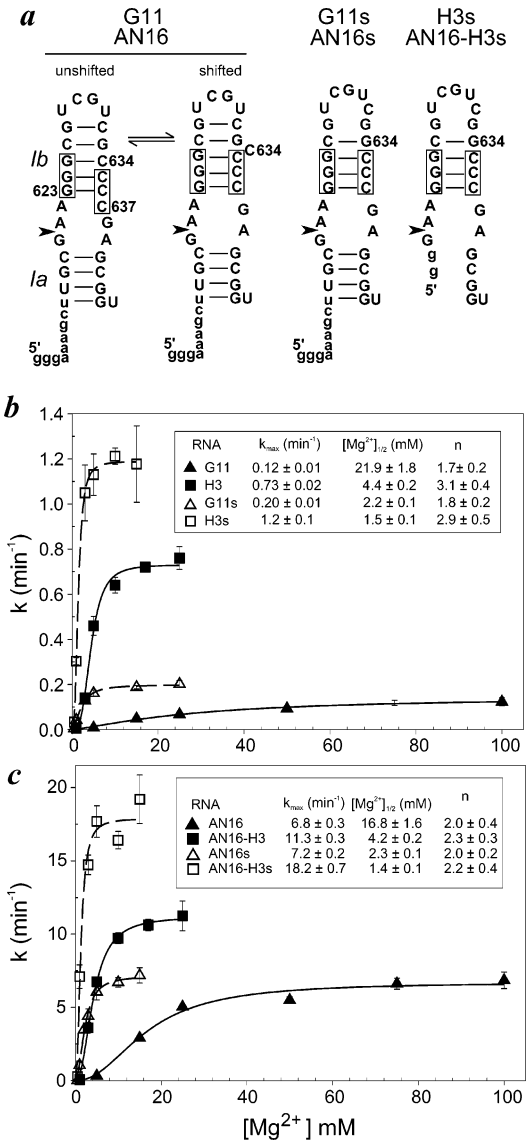

FIGURE 4: Mutations that favor the shifted conformation of stem-loop I lower the Mg^{2+} requirement for self-cleavage. (a) Secondary structures of mutant versions of stem-loop I. Helix Ia is disrupted in H3-based RNAs. Stem-loop I is mutationally locked in the shifted conformation by a C634G substitution in RNAs, whose name ends in s. In AN16-based RNAs, stem-loop I is attached to the rest of the ribozyme via a 16 nt linker (Figure 2a). (b, c) Cleavage rate constants, *k*, were measured over a range of Mg^{2+} concentrations and plotted and analyzed as in Figure 2.

sible for the high Mg^{2+} requirement of the latter RNAs. To test this idea, we disrupted helix Ia in the AN16 linker insertion mutant by changing the nucleotides upstream of the cleavage site to GGG, as had been done to disrupt helix Ia in the construction of H3 (cf. Figures 1a and 2a). We predicted that this mutant, called AN16-H3, would have a low $[Mg^{2+}]_{1/2}$ like that of H3, and possibly a slightly faster cleavage rate than AN16 because of the slight increase in effective linker length that results from unpairing the 3′ side of helix Ia. The data in Figure 3 show that both predictions were correct. The k_{max} of AN16-H3 was slightly higher than that of AN16 (11.3 vs 6.8 min^{-1}), and the disruption of helix Ia decreased the $[Mg^{2+}]_{1/2}$ from 16.8 mM in AN16 to 4.2 mM in AN16-H3, indistinguishable from that of H3 (4.4 mM). Taken together, the data in Figures 1−3 provide evidence that helix Ia is the structural feature responsible for determining the Mg^{2+} requirement and the length of the linker between helices Ia, and II determines the apparent cleavage rate.

Stabilizing the Shifted Conformation of Stem-Loop I by Mutation Lowers the Magnesium Requirement. We have previously shown that stem-loop I undergoes a conformational change in the presence of magnesium that is essential for cleavage of the wild-type VS sequence ((*14*); diagrammed in Figure 1b and 4a). The cleavable conformation has been called the shifted conformation because bases 623−625 on the 5′ side of helix Ib shift their pairing partners from 634 to 636 in the inactive, unshifted conformation to 635−637 in the active conformation. Also, some of the nucleotides in the internal loop that contains the cleavage site change their non-Watson−Crick interactions, as this loop changes from a symmetric six nucleotide loop to an asymmetric five nucleotide loop. The presence of helix Ia would be expected to stabilize the symmetric inactive conformation of the internal loop by stacking of the nucleotides in the cleavage site loop on helix Ia. Thus, helix Ia may contribute to a slow cleavage rate by stabilizing an inactive conformation, making it more difficult for stem-loop I to adopt the active shifted conformation.

If the low $[Mg^{2+}]_{1/2}$ values of H3 and AN16-H3 were due to ease of formation of the shifted conformation of stem-loop I, we hypothesized that cleavage reactions of RNAs that contained helix Ia might exhibit a lower $[Mg^{2+}]_{1/2}$ if stem-loop I were forced to adopt the shifted conformation by mutation. We have previously identified mutant sequences of helix Ib that form the shifted conformation even in the presence of helix Ia and irrespective of the presence or absence of Mg^{2+} (*14*). For example, MFOLD (*15*) predictions, chemical structure probing, and mutational analyses indicate that RNAs with a C634G substitution constitutively form the shifted conformation (*14*, *16*). We incorporated a C634G substitution to construct shifted mutants G11s and AN16s (Figure 4a). In addition, we constructed H3s and AN16-H3s to determine whether the effect of disrupting helix Ia and constitutively shifting stem-loop I might be additive. Cleavage rates were measured over a range of Mg^{2+} concentrations, and the k_{max} and $[Mg^{2+}]_{1/2}$ values are summarized in Figure 4b and c. Maximal cleavage rates (k_{max}) were affected very little (1.1 to 1.7-fold increase) in any of the shifted mutants compared to those of their parent RNAs; this suggests that adopting the shifted conformation of stem-loop I is not a significant rate-limiting step in the reaction pathway of any of these RNAs under these reaction conditions. Consistent with our hypothesis, $[Mg^{2+}]_{1/2}$ values were substantially lower for the shifted mutants compared to those of their parent RNAs: 10-fold for G11s vs G11 and 7-fold for AN16s vs AN16. Similar results were obtained with a different mutant of stem-loop I that also adopts the shifted conformation (containing double substitutions of G625C and C635G; data not shown). Mutants H3 and AN16-H3, which already lacked helix Ia, showed a further decrease in $[Mg^{2+}]_{1/2}$ values (about 3-fold) when the C634G substitution was also incorporated (see H3s and AN16s in Figure 4b and c). These data support the hypothesis that structural features that favor the shifted conformation of stem-loop I contribute to lowering the concentration of Mg^{2+} required for the cleavage reaction.

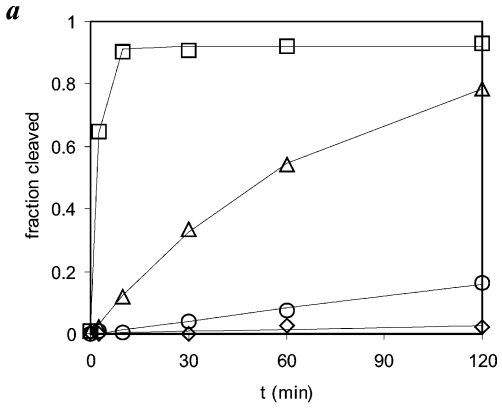

RNA	k_{max} (min^{-1})	$[Li^+]_{½}$ (M)	n
○ AN16	0.43 ± 0.01	1.7 ± 0.1	6.8 ± 0.6
△ AN16-H3	0.50 ± 0.01	1.2 ± 0.1	7.5 ± 1.0
□ AN16s	0.51 ± 0.01	0.9 ± 0.1	6.5 ± 1.0

FIGURE 5: Cleavage in monovalent cations. (a) Time course of the cleavage of AN16s (Figure 4a) in 40 mM TrisHCl at pH 8.0, 1 mM EDTA, and 3 M of the following monovalent salts: LiCl (□), NaCl (△), NH_4Cl (○), or KCl (◊). (b) Effect of LiCl concentration on self-cleavage rates of the indicated RNAs. k_{max} is the estimated cleavage rate at saturating LiCl, $[Li^+]_{1/2}$ is the concentration of LiCl required to obtain half-maximal cleavage rate, and *n* is the Hill coefficient.

Cleavage of Shifted RNAs Also Exhibits a Lower Ionic Concentration Requirement in Reactions Mediated by Monovalent Cations. Several of the small ribozymes, including VS, do not have an absolute requirement for Mg^{2+}, or even for divalent cations, in their cleavage reactions (*17*). Using a trans-acting version of the VS ribozyme, Murray et al. (*18*) observed activity in the presence of high concentrations of Li^+. We have confirmed and extended those results using cis-cleaving VS ribozymes. Figure 5a shows that LiCl and NaCl support efficient cleavage of AN16s (and other versions of the VS ribozyme, data not shown); cleavage was also seen with NH_4Cl but was barely detectable with KCl. Figure 5b shows the cleavage rates of AN16, AN16-H3, and AN16s measured over a range of Li^+ concentrations. The concentration of Li^+ required for each of these RNAs to reach half-maximal cleavage rate, $[Li^+]_{1/2}$, followed the same trend as that seen with Mg^{2+} (cf. Figure 4): wild-type AN16 required the highest cation concentration, AN16-H3 in which helix Ia is disrupted, required less, and AN16s in which stem-loop I constitutively adopts the shifted conformation required the lowest concentration. Also as seen in Mg^{2+}, the maximal cleavage rates in Li^+ of AN16s and AN16-H3 were only slightly faster than that of AN16, and the Hill coefficients, *n*, for all three RNAs were similar to each other (although $n \approx 7$ in Li^+ vs $n \approx 2$ in Mg^{2+}). Thus, the effects of linker insertion, disruption of helix Ia, and adopting the shifted conformation of stem-loop I on the ionic concentration requirement are not specific to cleavage reactions in Mg^{2+} but appear to reflect inherent properties of the RNAs.

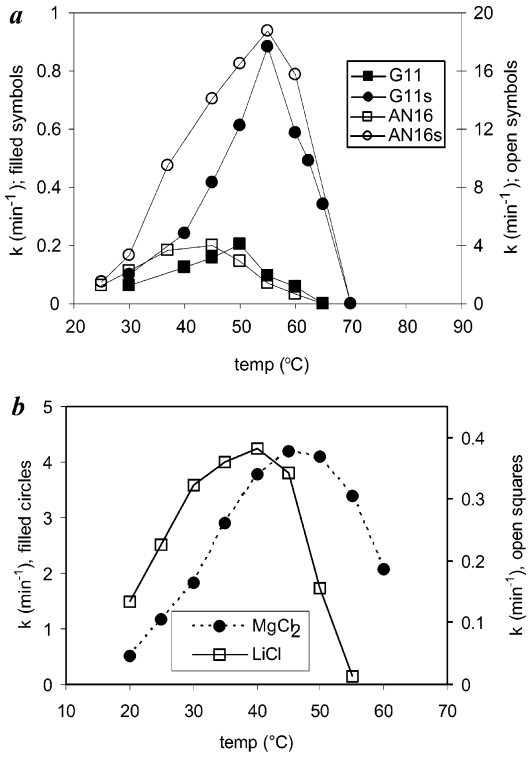

FIGURE 6: RNAs with low cation concentration requirements are also more thermostable. (a) Self-cleavage reactions were performed in a standard reaction mixture (Figure 2b) over a range of temperatures, and apparent first-order self-cleavage rate constants, *k*, were calculated. (b) Effect of temperature on the cleavage rate of AN16 in reaction mixtures containing 4 M LiCl or 50 mM $MgCl_2$. See Figures 1, 2, and 4 for the description of mutant RNAs.

The lower $[Mg^{2+}]_{1/2}$ and $[Li^+]_{1/2}$ of the RNAs that contain a constitutively shifted helix Ia suggested that the active conformations of these RNAs might be more stable, relative to that of other conformations, than was the case for their parent RNAs. To examine this possibility, we measured cleavage rates over a range of temperatures. Figure 6a shows that the cleavage rate of G11 increased only slightly with temperature, reaching its maximum at approximately 50 °C and decreasing to undetectable by 65 °C. In contrast, G11s showed a large increase in cleavage rate up to 55 °C, and it retained substantial activity even at 65 °C. AN16s, a linker-containing version of G11s, showed a similar trend, reaching a maximal cleavage rate of $\approx$ 20 min^{-1} at 55 °C, approximately 10° above the temperature optimum of AN16. The higher temperature optima and lower Mg^{2+} requirement of the RNAs with a shifted stem-loop I are consistent with the active conformations of these RNAs being more stable than their wild-type counterparts. This could be due to destabilization of inactive ground state structures or to stabilization of the transition state. For a given RNA (AN16 is shown as an example in Figure 6b), the temperature optimum and the maximal cleavage rate are higher in Mg^{2+} than in Li^+, consistent with divalent ions being more effective in favoring the active conformation.

Separating Stem-Loop I from the Ribozyme Core Mimics the Natural Cleavage Preference of VS RNA. The minimal

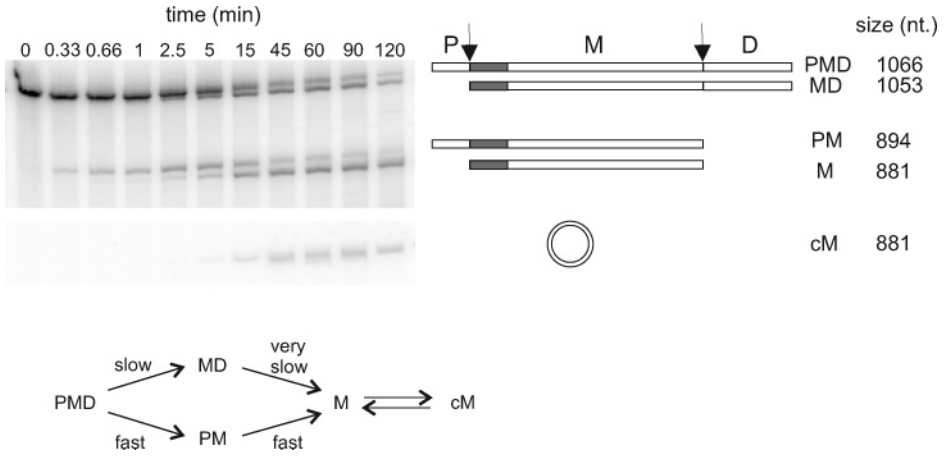

FIGURE 7: Partial dimer of VS RNA reveals a preference for cleavage at a site separated from the ribozyme core by a natural linker sequence. The RNA called PMD, synthesized by *in vitro* transcription of the clone GAv3′Ia, is shown schematically. PMD contains two copies of the self-cleavage site (arrowheads) and one copy of the ribozyme core (filled rectangle) in their natural context. Complete self-cleavage produces a T7-promoter-proximal fragment, P, a promoter-distal fragment, D, and a full-length VS monomer, M, which can self-ligate to produce circular monomer, cM of the sizes indicated; the diagram is not to scale. (See Supporting Information for the complete sequence of GAv3′Ia.) The time course of self-cleavage of PMD RNA in 40 mM Tris HCl at pH 8.0, 50 mM KCl, 2 mM spermidine, and 25 mM $MgCl_2$, separated by electrophoresis for 16 h at 1000 V on a 43 cm × 30 cm gel containing 4% polyacrylamide (40:2 acrylamide/bis) and 8 M urea; 1X TBE is shown to the left. The region of the image containing the circular monomer RNA, cM, which runs anomalously slowly on denaturing polyacrylamide gels, is shown under the main image. The small cleavage products P (13 nt) and D (168 nt) were run off the gel to facilitate resolution of the larger RNAs. The kinetic scheme shows the relative rates of cleavage at the upstream and downstream sites deduced from the appearance and disappearance of bands during the time course.

contiguous self-cleaving region of VS RNA identified by deletion experiments contains the cleavage site in stem-loop I located immediately upstream of the ribozyme core, as in the G11 construct (*11*). However, because natural VS RNA is a head-to-tail multimeric series of RNAs, a given ribozyme core sequence is also followed by another copy of stem-loop I approximately 0.7 kb downstream. We have found that tethering stem-loop I to the downstream end of the ribozyme core via a linker leads to increased cleavage rate (*8*), and the data presented above reinforce the idea that cleavage is faster when the distance between stem-loop I and the rest of the ribozyme is increased.

To test whether the ribozyme in its natural context prefers to cleave a site that is distant from the core, we constructed a partial dimer of VS RNA that contained one ribozyme core and two copies of stem-loop I, each in their natural location: one immediately upstream of the core and a second copy attached to the natural 0.7 kb sequence that comprises the rest of VS RNA (Figure 7). Different lengths of cloning vector sequence were appended to the 5′ and 3′ ends to endow the cleavage products with distinguishable electrophoretic mobilities. Cleavage at the upstream site would yield two products, designated P and MD; cleavage at the downstream site yields PM and D; and cleavage at both sites yields three products, P, M, and D. In a time course of self-cleavage (Figure 7), PM appears much sooner than MD, showing that the ribozyme preferentially cleaves the downstream site, that is, the site that is separated from the core by a long (0.7 kb) linker.

After cleavage at the downstream site to produce PM, the concentration of this RNA decreases, reflecting cleavage at its upstream site to liberate the natural linear monomer, M. M self-ligates to produce the circular monomer RNA, cM, as described previously (*19*). The small fraction of PMD that cleaves first at the upstream site, producing MD, cleaves slowly if at all at the downstream site, resulting in an accumulation of MD. The slow cleavage of MD may be due to the cleaved upstream stem-loop Ib, continuing to occupy the active site of the ribozyme after cleavage, thereby preventing the ribozyme from cleaving the downstream site. Consistent with this interpretation, a trans-acting version of VS (the Ava ribozyme) efficiently cleaves a separate stem-loop I substrate (*9*), whereas a similar ribozyme that contains stem-loop Ib (e.g., G11D, the self-cleavage product of G11, see Figure 1) works very poorly in trans (Oilve, J. E., and Collins, R. A., unpublished observation). Taken together, these observations show that cleavage in the natural VS RNA occurs preferentially at the site separated from the ribozyme core by a linker sequence.

CONCLUSION

We find that insertion of a linker sequence between stem-loop I and the rest of the ribozyme increases the cleavage rate by more than an order of magnitude (G11 vs AN16: 45-fold; H3 vs AN16-H3: 15-fold) with little or no effect (1.8-fold or 1.04-fold, respectively) on the $[Mg^{2+}]_{1/2}$. Linker-containing RNAs with mutations in helix Ib that constitutively adopt the shifted conformation required for activity, cleave at the same rate as the corresponding non-linker RNAs, but the Mg^{2+} requirement is lower by an order of magnitude (G11 vs G11s: 12-fold; AN16 vs AN16s: 7-fold). Disruption of helix Ia effectively converts the nucleotides formerly comprising the 3′ side of helix Ia into a short linker and favors the formation of the shifted conformation of helix Ib by eliminating a structural constraint. The effects of linker insertion, disruption of helix Ia, and constitutively adopting the shifted conformation are partially additive: the parental RNA, G11, cleaves with a maximal rate constant of 0.12 min^{-1} and a $[Mg^{2+}]_{1/2}$ of 21.9 mM, whereas an RNA containing all three of these alterations, AN16s, cleaves at 18 min^{-1} with a $[Mg^{2+}]_{1/2}$ of only 1.4 mM. These data show

that as with the hammerhead, hairpin, and HDV ribozymes, appropriate versions of the VS ribozyme are capable of efficient catalysis in the physiological range of Mg^{2+} concentrations. This raises the possibility that the activities of the small ribozymes may be regulated by the intracellular ionic environment, as has recently been reported for a Mg^{2+}-regulated RNA structural element in the 5′ untranslated region of a bacterial mRNA (*20*).

Interpreting the effect of a particular structural element on reaction kinetics can be challenging. For example, the presence of helix Ia inhibits cleavage at the site immediately upstream of the ribozyme core (as in the G11 construct); however, helix Ia is required for maximal cleavage rate in fast-cleaving constructs like RS19, where the cleavage site is tethered by a linker to the downstream of the ribozyme core (*8*). Helix Ia also shifts the cleavage−ligation equilibrium in favor of ligation in linker-containing RNAs (*8*). In hammerhead ribozymes, nonessential structural features can also affect the rates of cleavage and ligation as well as the ionic concentration requirements (*4*, *5*, *21*, *22*). In other ribozymes, for example, Group I introns (*23*, *24*) and RNase P (*25*), mutations that disrupt particular secondary structure elements or artificial circular permutations that change their relative locations have also been shown to influence the cleavage rate and/or folding pathway of the RNA. In VS RNA, helix Ia may have evolved to control the relative cleavage rates at the upstream and downstream sites.

SUPPORTING INFORMATION AVAILABLE

The complete sequence of GAv3′Ia. This material is available free of charge via the internet at http://pubs.acs.org.

REFERENCES

1. Lilley, D. M. (2005) Structure, folding and mechanisms of ribozymes, *Curr. Opin. Struct. Biol. 15*, 313−323.
2. Murchie, A. I., Thomson, J. B., Walter, F., and Lilley, D. M. (1998) Folding of the hairpin ribozyme in its natural conformation achieves close physical proximity of the loops, *Mol. Cell. 1*, 873−881.
3. Walter, N. G., Burke, J. M., and Millar, D. P. (1999) Stability of hairpin ribozyme tertiary structure is governed by the interdomain junction, *Nat. Struct. Biol. 6*, 544−549.
4. Khvorova, A., Lescoute, A., Westhof, E., and Jayasena, S. (2003) Sequence elements outside the hammerhead ribozyme catalytic core enable intracellular activity, *Nat. Struct. Biol. 10*, 708−712.
5. Penedo, J. C., Wilson, T. J., Jayasena, S. D., Khvorova, A., and Lilley, D. M. (2004) Folding of the natural hammerhead ribozyme is enhanced by interaction of auxiliary elements, *RNA 10*, 880−888.
6. Beattie, T. L., and Collins, R. A. (1997) Identification of functional domains in the self-cleaving *Neurospora* VS ribozyme using damage selection, *J. Mol. Biol. 267*, 830−840.
7. Rastogi, T., and Collins, R. A. (1998) Smaller, faster ribozymes reveal the catalytic core of *Neurospora* VS RNA, *J. Mol. Biol. 277*, 215−224.
8. Zamel, R., Poon, A., Jaikaran, D., Andersen, A., Olive, J., De Abreu, D., and Collins, R. A. (2004) Exceptionally fast self-cleavage by a Neurospora Varkud satellite ribozyme, *Proc. Natl. Acad. Sci. U.S.A. 101*, 1467−1472.
9. Guo, H. C., and Collins, R. A. (1995) Efficient trans-cleavage of a stem-loop RNA substrate by a ribozyme derived from neurospora VS RNA, *EMBO J. 14*, 368−376.
10. Lafontaine, D. A., Wilson, T. J., Norman, D. G., and Lilley, D. M. (2001) The A730 Loop is an important component of the active site of the VS ribozyme, *J. Mol. Biol. 312*, 663−674.
11. Guo, H. C., De Abreu, D. M., Tillier, E. R., Saville, B. J., Olive, J. E., and Collins, R. A. (1993) Nucleotide sequence requirements for self-cleavage of Neurospora VS RNA, *J. Mol. Biol. 232*, 351−361.
12. Milligan, J. F., Groebe, D. R., Witherell, G. W., and Uhlenbeck, O. C. (1987) Oligoribonucleotide synthesis using T7 RNA polymerase and synthetic DNA templates, *Nucleic Acids Res. 15*, 8783−8798.
13. Hiley, S. L., and Collins, R. A. (2001) Rapid formation of a solvent-inaccessible core in the Neurospora Varkud satellite ribozyme, *EMBO J. 20*, 5461−5469.
14. Andersen, A. A., and Collins, R. A. (2000) Rearrangement of a stable RNA secondary structure during VS ribozyme catalysis, *Mol. Cell. 5*, 469−478.
15. Zuker, M. (2003) Mfold web server for nucleic acid folding and hybridization prediction, *Nucleic Acids Res. 31*, 1−10.
16. Andersen, A. A., and Collins, R. A. (2001) Intramolecular secondary structure rearrangement by the kissing interaction of the Neurospora VS ribozyme, *Proc. Natl. Acad. Sci. U.S.A. 98*, 7730−7735.
17. Fedor, M. J. (2002) The role of metal ions in RNA catalysis, *Curr. Opin. Struct. Biol. 12*, 289−295.
18. Murray, J. B., Seyhan, A. A., Walter, N. G., Burke, J. M., and Scott, W. G. (1998) The hammerhead, hairpin and VS ribozymes are catalytically proficient in monovalent cations alone, *Chem. Biol. 5*, 587−595.
19. Saville, B. J., and Collins, R. A. (1991) RNA-mediated ligation of self-cleavage products of a Neurospora mitochondrial plasmid transcript, *Proc. Natl. Acad. Sci. U.S.A. 88*, 8826−8830.
20. Cromie, M., Shi, Y., Latifi, T., and Groisman, E. (2006) An RNA sensor for intracellular Mg^{2+}, *Cell 125*, 71−84.
21. Canny, M. D., Jucker, F. M., Kellogg, E., Khvorova, A., Jayasena, S. D., and Pardi, A. (2004) Fast cleavage kinetics of a natural hammerhead ribozyme, *J. Am. Chem. Soc. 126*, 10848−10849.
22. Nelson, J. A., Shepotinovskaya, I., and Uhlenbeck, O. C. (2005) Hammerheads derived from sTRSV show enhanced cleavage and ligation rate constants, *Biochemistry 44*, 14577−14585.
23. Heilman-Miller, S. L., and Woodson, S. A. (2003) Perturbed folding kinetics of circularly permuted RNAs with altered topology, *J. Mol. Biol. 328*, 385−394.
24. Woodson, S. A. (2005) Structure and assembly of group I introns, *Curr. Opin. Struct. Biol. 15*, 324−330.
25. Sosnick, T. R., and Pan, T. (2004) Reduced contact order and RNA folding rates, *J. Mol. Biol. 342*, 1359−1365.
26. Hoffmann, B., Mitchell, G. T., Gendron, P., Major, F., Andersen, A., and Collins, R. A. (2003) NMR structure of the active conformation of the Varkud satellite ribozyme cleavage site, *Proc. Natl. Acad. Sci. U.S.A. 100*, 7003−7008.
27. Michiels, P. J., Schouten, C. H., Hilbers, C. W., and Heus, H. A. (2000) Structure of the ribozyme substrate hairpin of Neurospora VS RNA: a close look at the cleavage site, *RNA 6*, 1821−1832.
28. Flinders, J., and Dieckmann, T. (2001) A pH controlled conformational switch in the cleavage site of the VS ribozyme substrate RNA, *J. Mol. Biol. 308*, 665−679.

BI060769+